Acta Oecologica **118** *(2023) 103889*
doi:10.1016/j.actao.2023.103889
a Malthusian Relativity paper

$\iota^{**}=7/3\psi$
mrLife.org

On the natural selection of body mass allometries

Lars Witting
Greenland Institute of Natural Resources, Box 570, DK-3900 Nuuk, Greenland. Email:lawi@natur.gl

Abstract I use data based life history models to illustrate natural selection causes for the evolution of inter-specific body mass allometries in birds and mammals. This illustrates *i*) how the primary selection of resource handling and mass-specific metabolism generates net energy for individuals, *ii*) how the selected net energy generates a population dynamic feedback selection where intra-specific interactive competition selects body masses that scale in proportion with net energy on the timescale of natural selection, *iii*) how the feedback selection of body mass buffers ecological variation in survival, *iv*) how the exponents of body mass allometries are selected from the dominant spatial dimensionality of the foraging ecology, *v*) how the population density allometry is affected by inter-specific competition, and *vi*) how primary selected metabolism bends the metabolic allometry and explains a metabolic invariance across major taxa of vertebrates.

Keywords: Natural selection, biological scaling, life history, foraging ecology, metabolism

1 Introduction

Allometry—the study of biological scaling—examines how the phenotypic traits (x) of organisms change

$$x = x_\circ w^{\hat{x}}, \tag{1}$$

in proportion with mass (w), with the exponent ($\hat{x}$; also power) being the slope, and $\ln x_\circ$ the intercept, on double logarithmic scale ($\ln x = \ln x_\circ + \hat{x} \ln w$).

A scaling with mass makes intuitive sense from a physiological point of view. For organisms with similar shapes, length tends to scale to the 1/3 power of mass, and area to the 2/3 power, reflecting the dimensional relationship between length, area, and volume. This made Rubner (1883) propose a 2/3 exponent for scaling between total metabolism and mass, as expected from a thermal homeostasis imposed by the ratio of surface area to volume. But an extra physiological dimension was needed (Blum 1977) to predict observed exponents that were closer to 3/4 than 2/3 (Kleiber 1932). A fractal physiological network was then proposed to endow life with the missing fourth dimension (West et al. 1997, 1999), with 3/4 power scaling suggested as a universal constant imposed by transportation constraints across surfaces of physiological networks.

Closer examinations showed however that there is no universal scaling as the allometric exponent depends on the scale of observation (e.g. Darveau et al. 2002; Niven and Scharlemann 2005; Glazier 2005, 2008, 2009; Duncan et al. 2007; White et al. 2007a,b, 2009; Sieg et al. 2009; Capellini et al. 2010; Killen et al. 2010; Kolokotrones et al. 2010). Examples include

i) 1/4 to 1/6 like transitions in the inter-specific exponents between terrestrial and pelagic species (Witting 1995, 2017a),

ii) a curvature where the inter-specific metabolic exponent of placental mammals increases from about 2/3 to more than 3/4 with an increase in mass (Kolokotrones et al. 2010; MacKay 2011),

iii) a decline in the inter-specific exponent of metabolism from prokaryotes over protist and protozoa to multicellular animals (Makarieva et al. 2008; DeLong et al. 2010),

iv) a transition from $-1/4$ like inter-specific scaling of mass-specific metabolism in major animal taxa to invariant scaling across taxa (Makarieva et al. 2005, 2008; Kiørboe and Hirst 2014), and

v) a change from about 3/4 to 3/2 in the allometric exponent for the rate of evolutionary increase in body mass covering the fossil record at different scales (Witting 2020).

The diverse allometric scaling supports the view that nothing in biology makes sense except in the light of evolution (Dobzhansky 1973). According to the natural selection paradigm, it is the naturally selected balance between metabolism and mass that defines their allometric relation, and this balance is evidently selected to different values dependent upon the scale of observation.

Today we have a large number of allometric theories that are perhaps more diverse than the exponents they attempt to explain (e.g. Witting 1995; West et al. 1997; Banavar et al. 1999; Kooijman 2000; Dodds et al. 2001; Dreyer and Puzio 2001; Banavar et al.

2002; Darveau et al. 2002; Rau 2002; Demetrius 2003; Fujiwara 2003; Makarieva et al. 2003; Santillán 2003; Glazier 2005; Ginzburg and Damuth 2008; Kozlowski et al. 2020; White et al. 2022). By acknowledging parsimony, I prefer the explanation with a minimum number of natural selection assumptions. This favours the population dynamic feedback selection that unfolds from the population growth of self-replication (Witting 1997, 2008, 2017b), a selection that links the natural selection of metabolism and body mass to the natural selection of the life history, foraging ecology, and body mass allometries as a whole. In addition to metabolism and body mass, this involves traits like resource handling, net energy, reproduction, survival, lifespan, population growth, abundance, and interactive competition, with the inter-specific allometric exponents following from the selected variation in mass (Witting 1995, 2017a).

To minimise uncertainty on evolutionary causality, the assumptions of population dynamic feedback selection do not include contingent trade-offs and constraints that evolve over time, allowing all traits to potentially evolve independently of one another (Witting 1997, 2008). Yet, energy conservation, self-replication, population growth, and competition in spatial habitats impose structural connections among the different life history and population ecological traits. It is this structure that defines how we build realistic population dynamic models, and as all living organisms are self-replicators, they can evolve only within the bounds of these population ecological constraints. This implies allometric exponents and transitions that follow from the intrinsic population ecological structure (Witting 1995, 2017a), as it is selected to evolve across different scales of observation, covering major life history transitions (Witting 2002, 2007, 2017b), inter-specific variation (Witting 1995), and body mass evolution in time (Witting 2018, 2020).

In the original work on population dynamic feedback selection I used mathematical equations to deduce the numerical values of allometric exponents from the evolutionary structure of my population ecological model (Witting 1995, 2017a). With this paper I plot inter-specific variation in the life history and ecology of birds and mammals to illustrate, and explain with a minimum of equations, some of the essential mechanisms behind the population dynamic feedback selection of metabolism, body mass, and allometries. This is done to show how the inter-specific variation that is usually plotted as allometries contain other correlations that reveal underlying selection mechanisms.

I start with an examination of the inter-specific variation in net energy that generates most of the variation in body mass before I examine the lack of evidence for r/k-selection. I then illustrate the presence of competitive interaction fixpoints, which are invariant selection attractors of interactive competition, discussing how the population dynamic feedback selection of the attractors buffer the natural selection of mass against the ecological variation in mortality.

My next focus is on the mass-rescaling selection that follows from the selection of mass, a process that selects for a decline in mass-specific metabolism and an associated dilation of natural selection time (Witting 2017a). The selected time dilation maximises the energy that is selected into mass and maintains the population dynamic growth and interactive competition of the population dynamic feedback selection of mass. I discuss how the selection of mass is entangled with the selection of optimal foraging, illustrating how the invariant selection attractor of interactive competition selects the dominant spatial dimensionality of the feeding ecology into the exponents of body mass allometries. The empirical and theoretical exponents are then compared discussing, among others, a relation between inter-specific competition and animal abundance. I then turn to the primary selection of mass-specific metabolism that explains a curvature for metabolic scaling in placentals and birds, as well as a metabolic invariance across major taxa of vertebrates. Relating to all these predictions at the end, I discuss why population dynamic feedback selection should be preferred over other allometric explanations.

2 Methods

I use 56,214 data estimates from the literature in my analysis of body mass allometries for the life histories of birds and mammals. The data were compiled into equilibrium life history models with zero population dynamic growth, with the relevant traits listed in Table 1. The details and equations that combine these traits into a population ecological model, including the development of the population dynamic feedback selection of the traits, are published elsewhere (Witting 1997, 2008, 2017a,b).

Missing parameters were calculated by inter-specific extrapolations by allometric correlations, following Witting (2021). Yet, I use only raw data, and derived traits that were calculated from data estimates of other traits, in the statistical calculations of correlations and exponents. Plots, however, are presented with parameter estimates for approximately 90% of all species of birds and mammals.

Taxonomies and names were obtained from Wilson

S	U	**Individual growth**
t_p	y	Pregnancy/incubation period
t_0	y	Age at birth/hatching, $t_0 = 0$
t_j	y	Age at weaning/fledging
t_i	y	Age of independence from parents
w	y	Adult body mass
$\acute{w}_x$	-	Relative mass $\acute{w}_x = w_x/w$ at $t_x \in \{t_0, t_j, t_i\}$

S	U	**Demographic traits**
t_m	y	Age of reproductive maturity
t_r	y	Expected reproductive period; $t_r = 1/q_{ad}$
t_g	y	Generation, average age of reproduction; $t_g = t_m + p_{ad}/q_{ad}$
t_l	y	Maximum lifespan
l_m	t_m^{-1}	Offspring survival from t_0 to t_m; $l_m = 2/R$
p_{ad}	y^{-1}	Annual adult survival
q_{ad}	y^{-1}	Annual adult mortality; $q_{ad} = 1 - p_{ad}$
m	y^{-1}	Offspring per female per year
R	t_r^{-1}	Expected lifetime reproduction; $R = t_r m$
λ^*	t_g^{-1}	Equilibrium growth rate $\lambda^* = l_m t_r m/2 = 1$

S	U	**Life history energetics**
$\underline{\beta}$	W/g	Basal mass-specific metabolism
$\overline{\beta}$	W/g	Field mass-specific metabolism
$\tilde{\beta}$	Hz	Metabolic pace $\tilde{\beta} = \beta/W$; frequency of 1 J work per g; $W = 1\mathrm{J/g}$
α	J	Resource handling; net assimilated energy per metabolic pace; $\alpha = \grave{\alpha}\rho$; $\grave{\alpha}$:intrinsic handling; ρ:resource density
ϵ	W	Net assimilated energy available for reproduction; $\epsilon = \alpha\tilde{\beta}$
ϵ_g	W	Gross assimilated energy; $\acute{\epsilon}_g = \epsilon_g/\epsilon$
w_ϵ	J	Adult body mass as combustion energy

S	U	**Population ecology**
N	km^{-2}	Population density
b	$\mathrm{kg/km}^2$	Biomass of population, $b = wN$
ϵ_n	$\mathrm{W/km}^2$	Energy consumed per population, $\epsilon_n = \epsilon_g N$
h	km^2	Home range of individual
h_o	-	Home range overlap $h_o = hN$
v	(Hz)	Relative frequency of competitive encounters per individual per h_o
I	(Hz)	Relative intra-specific interference competition per individual; $I \propto h_o v$. Rescaled to a log value ($\iota = \ln I$) of unity for the median in birds

Table 1: Symbols (S) and units (U) of estimated traits, with details in Witting (2021).

and Reeder (2005) for mammals and from Gill and Donsker (2014) for birds, and body masses were obtained primarily from Smith et al. (2004) for mammals and Dunning (2007) for birds. Primary data on basal metabolism were obtained from McNab (2008) for mammals and McKechnie and Wolf (2004) for birds, with field metabolic rates from Hudson et al. (2013). Data for parameters on reproduction, time periods, and individual growth were obtained from a variety of sources including Jetz et al. (2008), De Magalhães and Costa (2009), Jones et al. (2009), and Myhrvold et al. (2015). I conducted an independent literature search for annual survival rates across all major taxa of birds and mammals, with major data sources including McCarthy et al. (2008), DeSante and Kaschube (2009), Ricklefs et al. (2011), del Hoyo et al. (1992–2011), and Wilson and Mittermeier (2009–2014). Population densities were obtained from Damuth (1987) and Santini et al. (2018), and home range areas from Tucker et al. (2014), Tamburello et al. (2015), and Nasrinpour et al. (2017) with a separate literature search for bats and marine mammals. Some of the data in these publications are the same, and I determined the value of a trait for a species as the average of the available raw data,

resulting in more weight to commonly agreed estimates.

Some of the life history and ecological traits that are included in my analysis are not usually provided as data, so they were calculated as derived traits from other traits given the underlying population model. This involves the reproductive period $t_r = 1/q_{ad}$ that was calculated from adult annual mortality (q_{ad}), lifetime reproduction $R = t_r m$ that was calculated from the reproductive period and annual reproduction (m), and the probability that an offspring survives to the age of reproductive maturity that was calculated as $l_m = 2/R$ from the equilibrium constraint $\lambda^* = l_m R/2 = 1$ of zero population dynamic growth (eqn 3).

Body mass measured by combustion energy (SI unit J) was calculated as $w_\epsilon = c_{w\to d} c_{d\to\epsilon} w$ where w is mass in grams, $c_{w\to d}$ is the conversion of wet to dry organic matter [set to 0.40 for birds (Mahoney and Jehl 1984), and 0.35 for mammals (Prothero 2015)], and $c_{d\to\epsilon}$ is the conversion of dry organic matter to energy [set to 22.6 kJ/g based on Odum et al. (1965) and Griffiths (1977)]. These estimates were used to calculate net energy (ϵ) by the following equation $R = \epsilon t_r/\acute{\beta} w_\epsilon$ for lifetime reproduction, with ϵt_r being the net energy used for lifetime reproduction, and $\acute{\beta} = (w_i + t_e \beta \bar{w}_i)/w$ correcting for relative mass (w_i/w) at the age of independence (subscript i) and the relative energy metabolised by the offspring $(t_e \beta \bar{w}_i)/w$ during the period of parental care (t_e), with $\bar{w}_i$ being the average mass of the offspring during this period, calculated from a Gompertz (1832) growth equation that passed through body mass estimates at the age of birth/hatching and age of weaning/fledging. Resource handling $\alpha = \epsilon/\beta$ was then estimated from net energy and field mass-specific metabolism.

Higher level ecological traits included home range overlap $h_o = hN$ calculated from the home range divided by the average space availability ($1/N$), with the latter given by the inverse of the population density per unit habitat. A relative measure of the frequency of competitive encounters per individual per unit home range overlap was calculated as $v \propto v_f/l_f$, where $l_f \propto h^{1/d}$ is the length of foraging tracks (assumed proportional to the dth root of the d-dimensional home range) and $v_f \propto \beta_\beta w^{1/2d}$ is the average speed of foraging on those tracks, as expected from allometric correlations with β_β being the intercept of the metabolic allometry $\beta = \beta_\beta w^{-1/2d}$ (Witting 1995, 2017a). The level of intra-specific interference competition per individual was approximated as a relative measure $I \propto h_o v \propto Nhv$ obtained by multiplying the home range overlap with the frequency of competitive encounters per individual per unit home range overlap. All estimates of I were rescaled to obtain a log value ($\iota = \ln I$) of unity for the median across all species of birds. See Witting (2021) for additional details on estimation.

Having the different traits estimates, I use double logarithmic scale to estimate traits correlations and inter-specific allometric exponents by linear regression. For some comparisons involving derived traits the dependent and independent traits are not statistically independent, with the estimated correlations and exponents being approximations only. Yet, my purpose with this study is not to claim statistical relations for traits across natural population. It is only to show that the correlations of the available data are consistent with population dynamic feedback selection also when compiled into traits that are usually not estimated for natural populations but are essential for our understanding of the underlying selection.

Owing to major life history differences I split mammals into placentals (minus bats), marsupials and bats, while all birds are analyses together. Statistical correlations are calculated mainly for birds and placentals, as there are often too few data for marsupials and bats. The dominant spatial dimensionality of the foraging ecology follows the data-based classification in Witting (2017a). All birds, bats, and marsupials are classified as having 2D ecology, while few taxa of placentals are classified with 3D ecology [Cetaceans, Primates, and the three Carnivora families Otariidae, Odobenidae, and Phocidae]. A selected set of inter-specific trait correlations are plotted in Fig. 1 for birds and placentals, and in Fig. 2 for marsupials and bats. In the sections below I refer collectively to plots of the same parameters (marked by identical letters) across the four taxonomic groups in the two figures.

3 Net energy, mass, & allometry

Net energy (ϵ)—i.e. the energy organisms have available for reproduction—is one of the most essential traits in natural selection. It is not only exposed to primary selection for an exponential increase due to the direct link to fitness through the rate of replication, but it is also the primary driver of population growth and the associated population dynamic feedback selection (Witting 1997).

Independently of the actual selection of mass we expect quite generally a body mass that is proportional to net energy on the natural selection timescale of the species

$$w \propto t_r \epsilon \tag{2}$$

with the reproductive period $t_r \propto 1/\beta$ being inversely related to the pace-of-life (Pearl 1928), as defined by

mass-specific metabolism (β). The corresponding $w \propto \epsilon/\beta$ relation is illustrated in the a-plots [theoretical exponent of 1; observed of 0.92 (se:0.04; n:32) for birds & 1.00 (se:0.03; n:64) for placentals], and it is perhaps most easily recognised from a population dynamic growth rate

$$\lambda^* = l_m R = l_m\, t_r \epsilon / 2\acute{\beta} w = 1 \tag{3}$$

that is constrained by the population dynamic equilibrium ($*$), with l_m being the probability that an offspring survives to the age of reproductive maturity, $R = t_r\epsilon/\acute{\beta}w$ being reproduction over the reproductive period, and $\acute{\beta}$ a body mass invariant adjustment for the relative mass and energy metabolised by offspring (for details on the life history model see Witting 2017a). With l_m being body mass invariant and t_r being inversely proportional to β, we obtain eqn 2 from eqn 3.

Following eqn 2, we may write the selected rate of change in body mass as a function of the selected change in net energy

$$\partial \ln w / \partial \ln \epsilon = 1/\hat{\epsilon} \tag{4}$$

where $\hat{\epsilon}$ is the exponent of the allometry for net energy ($\epsilon = \epsilon_\circ w^{\hat{\epsilon}}$). This selection of mass with inverse allometric causality illustrates that allometries—where traits are described as functions of mass—are not necessarily natural selection cause-and-effect relations.

Relating to cause and effect, we may define the mass-rescaling allometry of a trait x as the natural selection change that is imposed by a natural selection change in mass

$$\partial \ln x / \partial \ln w = \hat{x} \tag{5}$$

with the mass-rescaling response ($\partial \ln x/\partial \ln w$) being the mass-rescaling exponent ($\hat{x}$). The body mass imposed rate of change in the trait

$$\frac{d \ln x}{d\tau} = \frac{\partial \ln x}{\partial \ln w}\frac{d \ln w}{d\tau} \tag{6}$$

is thus ultimately a function of the selected change in net energy, with

$$\frac{d \ln x}{d\tau} = \frac{\partial \ln x}{\partial \ln w}\frac{\partial \ln w}{\partial \ln \epsilon}\frac{d \ln \epsilon}{d\tau} = \frac{\hat{x}}{\hat{\epsilon}}\frac{d \ln \epsilon}{d\tau} \tag{7}$$

with τ denoting the per-generation timescale of natural selection.

4 r/k-selection

Let us first consider the possibility that the selected allocation of energy between mass, replication, and allometries could be controlled by frequency-independent r/k-selection (Charlesworth 1971; Roughgarden 1971). Owing to the frequency-independence and the associated constancy of the relative fitness of a variant, r/k-selection has the special feature that the average fitness of a population is a trait that evolves just like any other phenotypic trait. This implies a constant increase in the average fitness of populations, as expressed by an increase in r or k (Fisher 1930).

A selection increase in net energy and body mass by r/k-selection is thus associated with an increase in the demographic traits, population dynamic growth rate, and density of the population, with an even stronger increase in the amounts of resources that are consumed by the population. There is no allometric support for this very basic prediction. There are instead declines in both r and k with an increase in mass (Fenchel 1974; Damuth 1981, 1987; Hatton et al. 2019), population densities that decline with an increase in net energy [b-plots, exponent: -0.78 (se:0.35; n:26) for birds & -1.21 (se:0.13; n:65) for placentals], and a consumption of energy by populations that are invariant of net energy in birds, but not in placentals where population consumption declines with increased net energy [c-plots, correlation: -0.06 (p:0.78; n:26) for birds & -0.23 (p:0.07; n:65) for placentals].

Another issue with r/k-selection relates to the quality-quantity trade-off $\lambda \propto \epsilon/w$ of eqn 3, where a few large or many small offspring can be produced from the same amount of energy (Smith and Fretwell 1974; Stearns 1992). This implies a replication rate that is inversely related to mass, with continued selection for a decline in mass. The existence of large organisms is simply not supported by basic r/k-selection, making it essential to identify another selection mechanism that will outbalance the frequency-independent selection for negligible mass.

5 Dynamic feedback selection

Population growth is the ultimate cause for the unfolding of a density-frequency-dependent population dynamic feedback selection of mass. The frequency-dependent resource monopolisation from the density-dependent interference competition selects for an increase in body mass, and this outbalances the frequency-independent selection for negligible mass (Witting 1997). The feedback selection is predicted to be fully developed at the evolutionary transition to multicellular animals, with the selection of mass among unicells being driven also by a metabolic mass-dependence that vanishes with the selection of fully developed metabolic pathways (Witting 2017b).

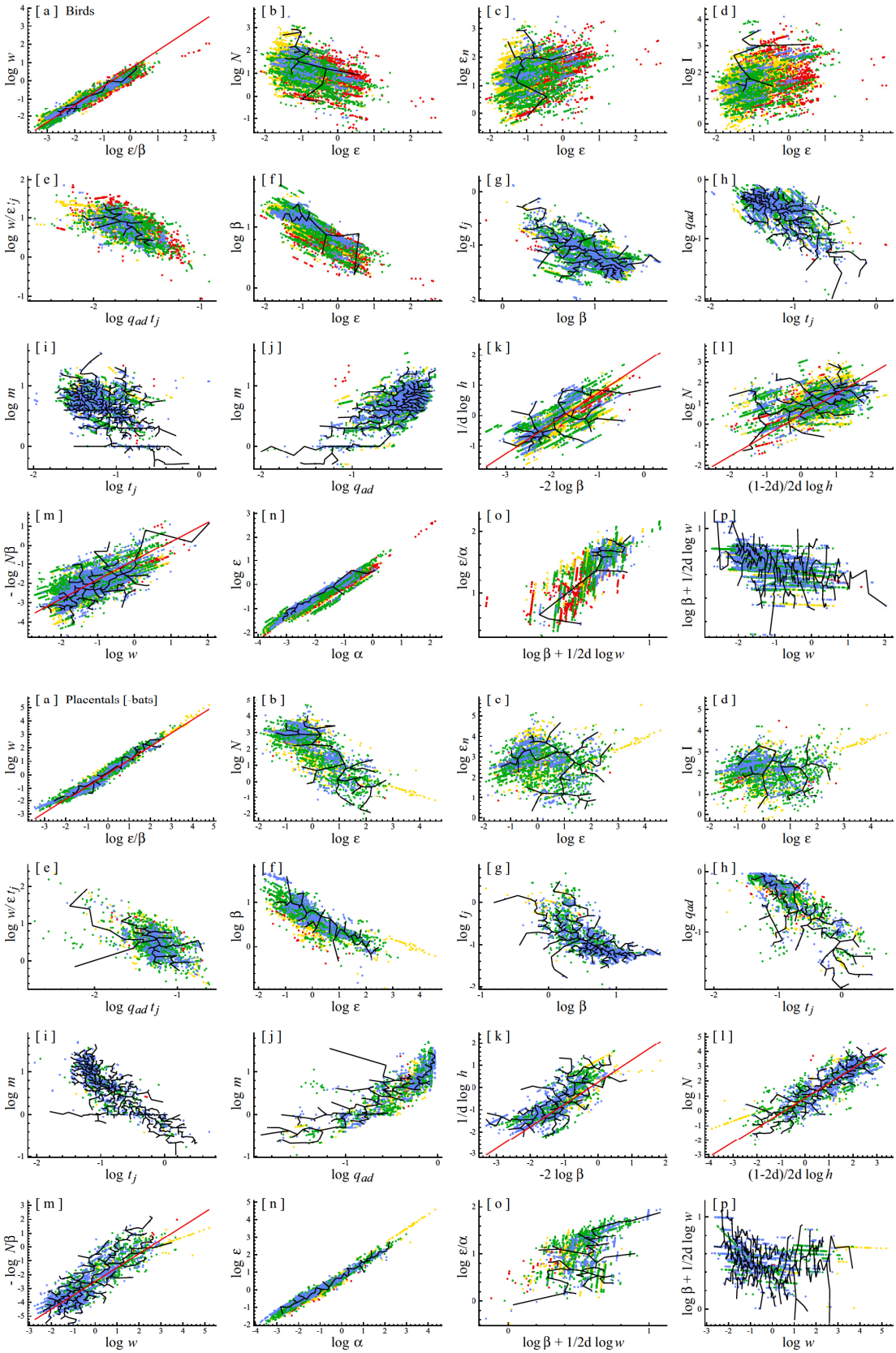

Figure 1: **Life history evolution.** Inter-specific trait correlations that illustrate the natural selection of life histories in birds (top 16 plots) and placentals (minus bats; bottom 16 plots). Black lines outline the space with data for both parameters, coloured dots estimates at different phylogenetic levels (defined by the highest estimation level for the two parameters), and red lines theoretical predictions of proportionality. Estimator levels: data (black), genus (blue), family (green), order (yellow), and class (red); with points of the latter sitting on top of the former.

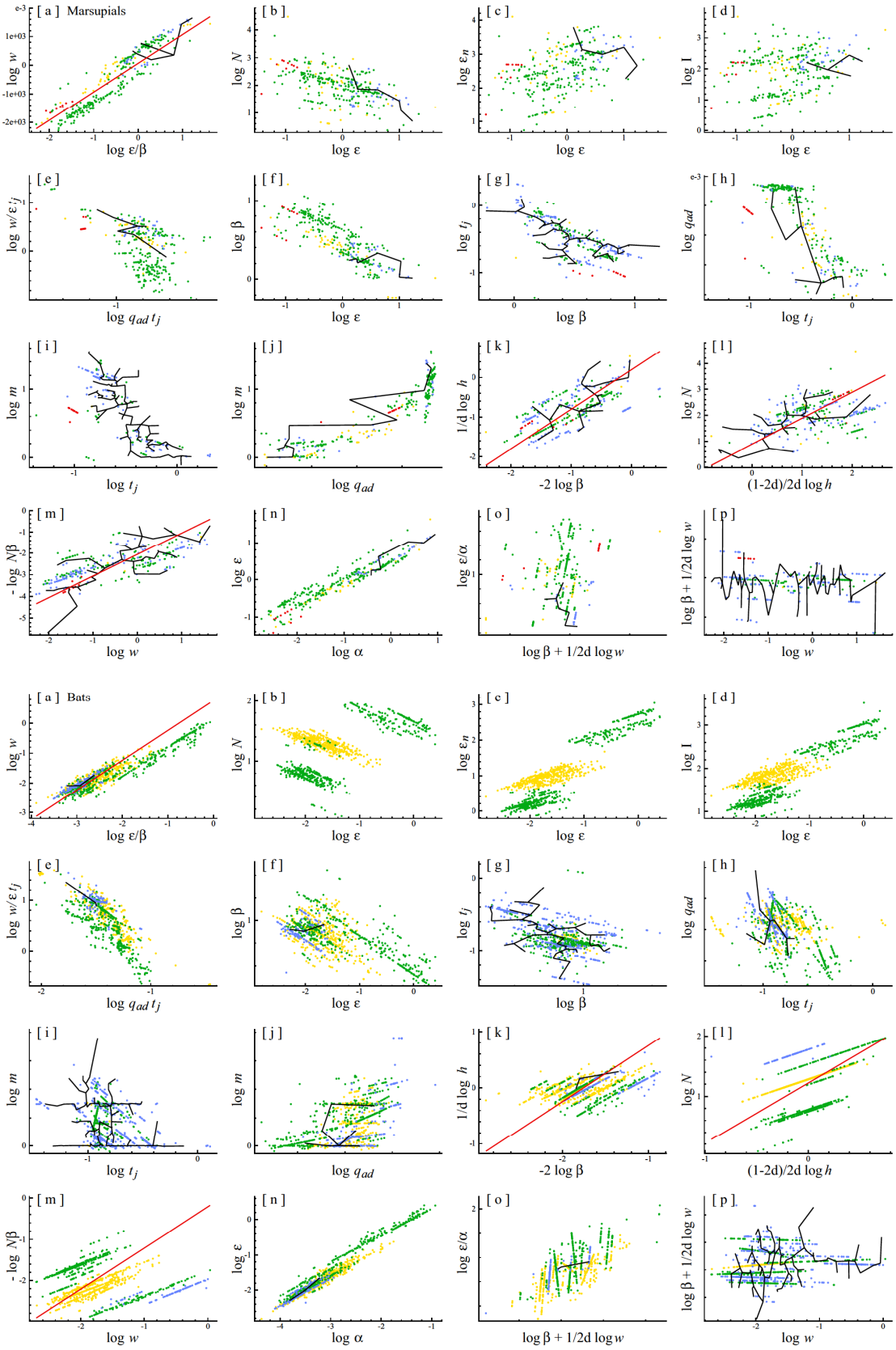

Figure 2: **Life history evolution.** Inter-specific trait correlations that illustrate the natural selection of life histories in marsupials (top 16 plots) and bats (bottom 16 plots). Black lines outline the space with data for both parameters, coloured dots estimates at different phylogenetic levels (defined by the highest estimation level for the two parameters), and red lines theoretical predictions of proportionality. Estimator levels: data (black), genus (blue), family (green), order (yellow), and class (red); with points of the latter sitting on top of the former.

The population dynamic feedback is actively balancing the density-frequency-dependent selection for an increase in mass against the frequency-independent selection for a decline in mass. The frequency-independent selection for a decline in mass and increase in r and k generates the population dynamic growth of the population, with the level of intra-specific interactive competition increasing with an increase in abundance. The increase in interference competition is then generating a density-frequency-dependent resource bias in favour of the competitively superior individuals, and when the bias becomes sufficiently strong it outbalances the selection of the quality-quantity trade-off selecting net energy into mass at the cost of the demographic traits. This allows for the evolution of a variety of body masses that reflect the underlying inter-specific variation in the net assimilated energy of species, with r and k being selected—as observed—to decline with a selection increase in net energy and body mass (Witting 1995).

The attractors of population dynamic feedback selection are competitive interaction fixpoints that maintain an invariant level of intra-specific interference by the selected allocation of net energy between reproduction and mass. By selecting the level of interference, the attractor is outbalancing the negative selection of the quality-quantity trade-off by adjusting the resource bias of interactive competition and the associated selection of mass.

The log of the average number of interactive encounters per individual (ι) at the competitive interaction fixpoint has a predicted value of

$$\iota^{**} = 1/\psi \tag{8}$$

when the body mass in selected to an evolutionary equilibrium ($**$), and a value of

$$\iota^{*s} = \frac{1}{\psi}\frac{4d-1}{2d-1} \tag{9}$$

when body mass is selected to increase exponentially at an evolutionary steady state ($*s$) with an exponential increase in net energy [Witting, 1997; ψ is the intra-population gradient (around the average life history) in the fitness cost of interference competition per unit interference (caused by differential resource access); d is the dominant number of spatial dimensions in the foraging ecology of the species].

The truly invariant component of the attractors is not the number of interactive encounters, but the intra-population fitness bias from interactive competition [$\iota^{**}\psi = 1$ & $\iota^{*s}\psi = (4d-1)/(2d-1)$]. To understand population dynamic feedback selection it is essential to understand that it are the population level gradients in resource assess by interactive competition ($\iota^{**}\psi$ & $\iota^{*s}\psi$) that are the core attractors of natural selection, with life history traits and foraging behaviour being naturally selected by the feedback mechanisms of the selection so that the population mechanistic bottom-up generation of intra-specific interference is adjusted to match the pre-determined value of the overall attractor.

With non-significant correlations between net energy and the estimated level of interference competition we do not falsify the existence of competitive interaction fixpoints [d-plots, correlation: 0.31 (p:0.28; n:14) for birds & -0.15 (p:0.33; n:41) for placentals].

6 Extrinsic mortality

The selection attractors of the competitive interaction fixpoints imply a feedback where increased extrinsic mortality selects for increased fecundity. This is imposed by the selection of invariant interference, where increased extrinsic mortality—and the associated decline in density and interference competition—selects an increase in fecundity until the interference competition of the competitive interaction fixpoint is re-established (Witting 1997, 2008).

The energy for a selection increase in fecundity is taken primarily from a selection decline in mass. Yet, a large component of the increase in yearly fecundity with increased yearly mortality follows from the body mass selected scaling of rates and periods (see next subsection). So, to analyse for the influence of extrinsic mortality, we examine the residual component where an allometrically independent increase in mortality selects for an increase in fecundity. The residual variation in body mass ($w/\epsilon t_j$)—relative to the mass expectation of the net assimilated energy ($w \propto \epsilon t_j \propto w^{\hat{e}+\hat{t}} \propto w^1$)—should thus be selected to decline with increased extrinsic mortality. This is illustrated in the e-plots where residual mass is declining significantly with a mortality rate ($q_{ad}t_j$) that is time-scaled to eliminate the allometric dependence [correlation: -0.76 ($p<0.001$; n:37) for birds & -0.57 ($p<0.001$; n:68) for placentals].

A decline in mass with an increase in natural or anthropogenic mortality has been identified for a variety of species (e.g., Reznick et al. 1996; Haugen and Vøllestad 2001; Sinclair et al. 2002; Carlson et al. 2007; Herczeg et al. 2009; Rossetto et al. 2012). The often-observed decline in mass following human-induced mortality is often argued to reflect a selective harvest for larger individuals (e.g., Browman 2000; Sinclair et al.

2002; Olsen et al. 2004). Yet, the importance of intraspecific mass-specific mortality is likely overstated in the literature as the base-case response of natural selection to increased mortality is a selection decline in mass.

7 Mass-rescaling selection

Why does natural selection scale the life history in response to evolutionary changes in body mass? One reason is metabolic trade-offs that are adjusted during the selection of mass (Witting 2017a). A selection increase in mass implies that the offspring metabolises more energy during the period of parental care. This additional metabolism is wasted energy from a fitness point of view, as it might instead be allocated to the increase in mass that is favoured by natural selection. Larger variants with a lower mass-specific metabolism are thus expected to have the highest fitness.

A mass-rescaling decline in mass-specific metabolism with an increase in mass, however, implies a smaller pace of resource handling and thus less net assimilated energy in physical time. Yet, if the variant has life-periods that scale inversely with metabolic pace, the decline in metabolism implies prolonged life-periods with net energy for the selected mass being maintained on the dilated timescale of natural selection. A downscaling of mass-specific metabolism, with an associated inversely proportional upscaling of biological periods, are thus maximising the energy that is available for the natural selection of mass on the timescale of natural selection.

This mass-rescaling is identified by a selection decline in mass-specific metabolism with an increase in the net energy that drives the natural selection of mass [f-plots, exponent: -0.36 (se:0.05; n:32) for birds & -0.32 (se:0.02; n:64) for placentals], and by an inverse scaling between mass-specific metabolism and biological periods [g-plots, exponent: -0.74 (se:0.05; n:255) for birds & -0.60 (se:0.04; n:409) for placentals].

The inverse scaling of rates and periods is reflected e.g. in a decline in yearly mortality [h-plots, exponent: -0.77 (se:0.03; n:492) for birds & -0.79 (se:0.05; n:171) for placentals] and fecundity [i-plots, exponent: -0.66 (se:0.02; n:1280) for birds & -0.98 (se:0.02; n:1273) for placentals] with increased life periods. The result is a strong positive correlation between yearly mortality and yearly fecundity [j-plots, exponent: 0.78 (se:0.03; n:512) for birds & 0.93 (se:0.04; n:165) for placentals].

Another consequence of mass-rescaling is reflected in the invariant population growth at the dynamic equilibrium of eqn 3, where body mass is selected proportional to ϵ/β as indicated by eqn 2 and illustrated by the a-plots [theoretical exponent of 1; observed of 0.92 (se:0.04; n:32) for birds & 1.00 (se:0.03; n:64) for placentals]. A body mass in proportion with ϵ/β does not indicate a particular numerical value for the scaling between metabolism and mass. In other words, the allometric exponents are not given by the constraints considered so far.

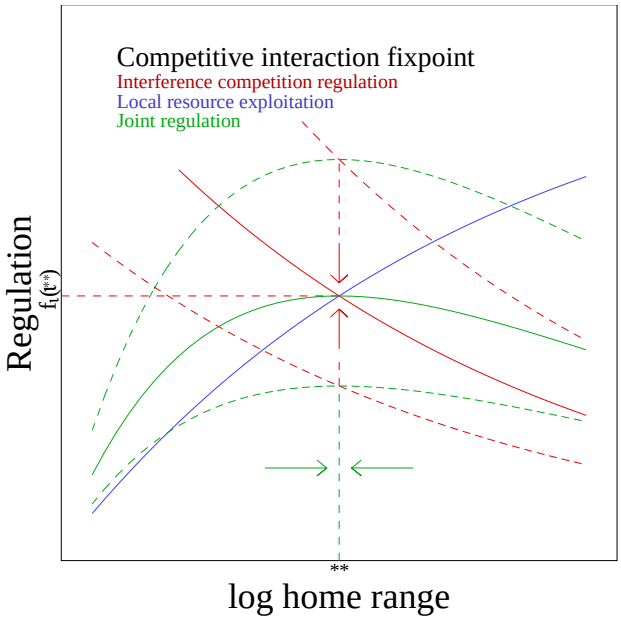

Figure 3: **Optimal foraging.** The home range of optimal density regulation (**) is defined by the selection attractor on the joint regulation ($f_s f_\iota$; green curves) of local resource exploitation (f_s; blue curve) and interactive competition (f_ι; red curves), with the latter [$f_\iota(\iota^{**})$] being selected to match the interactive competition (ι^{**}) of the selection attractor on body mass. From Witting (2017b).

8 Allometries from optimal foraging

With the selection attractor on body mass determining the level of interference competition in the population, the selection of mass is intrinsically linked to the ecological regulation of the foraging process that generates the net energy that drives the population dynamic feedback selection of mass. This link is so strong that the exponents of the mass-rescaling allometries follow from the spatial constraints on optimal foraging (Witting 1995, 2017a).

Optimal foraging is a balance between the cost (i.e. regulation) of local resource exploitation and the cost of interactive competition (Fig. 3). The former selects

for large home ranges to avoid an over-exploitation of the local resource, and the latter selects for small home ranges to avoid competitive encounters with other individuals in the overlapping areas of individual home ranges. The overall selection attractor is an invariant equilibrium where the trade-off between the two types of regulation are selected to a foraging optimum, with regulation (f) by interference [$f_\iota(\iota^{**})$] being selected also to the invariant selection attractor of interactive competition (Fig. 3). Owing to the selected balance, regulation by local resource exploitation (f_s) is a selected invariance also, and so is the amount of resources metabolised by the population (Witting 1995, 2017a,b).

These invariant regulation levels are ecological top-down constraints on the overall selection attractor. The regulations, however, are generated bottom-up by the foraging behaviour of the individuals in the population, with the natural selection solution being restricted to foraging patterns that generate the invariant regulation of the overall selection attractor. The prediction of the allometric exponents follow from the trait combinations of this ecologically constrained bottom-up foraging process, and the exponents may thus vary among species with vastly different foraging ecology. So far, I have developed the deduction only for an idealised situation where individuals compete for evenly distributed home ranges in one, two, and three spatial dimensions.

To analyse for the possible trait combinations that can generate the regulation of the overall selection attractor, we may deal with regulation as a multiplicative function on net energy (where $f = 1$ is no costs, and $f = 0$ maximal cost). Local resource exploitation [$f_s(\beta/v)$] may then be approximated as a monotonically increasing function of the period ($1/v$) between reuse of foraging tracks (v is pace of reuse) when scaled by the metabolic pace of the organism to obtain a relative function that reflects pace at the limit of infinitely large home ranges (Witting 1995, 2017a). The pace of track reuse ($v = v_f/l$) is foraging speed (v_f) divided by track length (l), with foraging speed on the body mass axis being inversely proportional to metabolic pace ($v_f \propto 1/\beta$; Garland 1983; Calder 1984). With track length scaling to the $1/d$th power of the home range because of the $A = L^2$ and $V = L^3$ relations between length (L), area (A), and volume (V), foraging speed scales as $v \propto 1/\beta h^{1/d}$ with regulation by local resource exploitation scaling as $f_s(\beta^2 h^{1/d})$.

As the $\beta^2 h^{1/d}$ argument of the f_s function is invariant at the selected foraging optimum, we expect a $h^{1/d} \propto \beta^{-2}$ relation where the dth root of the home range scale in proportion to the negative square of mass-specific metabolism [k-plots, theoretical exponent of 1;

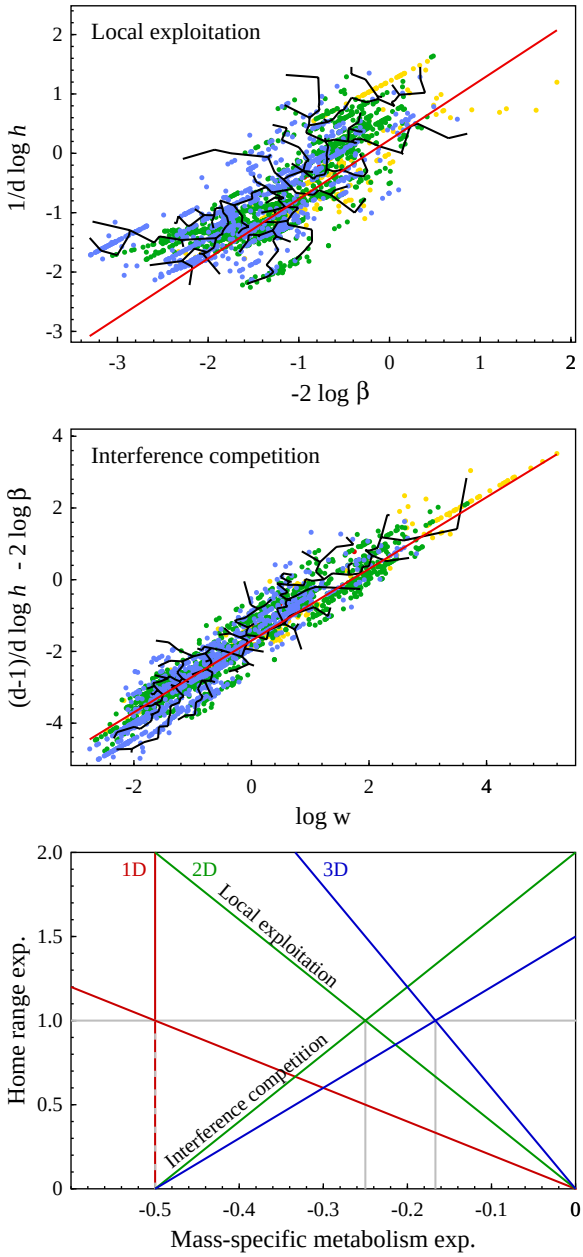

Figure 4: **Allometric deduction.** For placentals, the top and middle plots show allometric representations of the invariant regulations by local exploitation and interference competition, with the theoretical predictions (2 red lines) solved in the bottom plot for the mass-rescaling exponents $\hat{h}$ and $\hat{\beta}$ for home range and mass-specific metabolism. With $\hat{h}$ increasing with $\hat{\beta}$ for interference competition [$\hat{h} = d(1 + 2\hat{\beta})/(d-1)$] and declining for local exploitation [$\hat{h} = -2d\hat{\beta}$], the selected exponents [$\hat{h} = 1$ & $\hat{\beta} = -1/2d$] are the solutions with identical relations for $d \in \{1, 2, 3\}$.

observed of 0.57 (se:0.09; n:74) for birds, 0.84 (se:0.06; n:190) for placentals, & 0.89 (se:0.23; n:23) for marsupials]. This relation does not by itself give us a value for the scaling of metabolism and home range with body mass, but it gives us a scaling between home range and mass-specific metabolism, with the relation being dependent on the dominant dimensionality of the foraging ecology.

If we look at regulation by interactive competition we have $f_\iota(h_o v) = f_\iota(Nh^{(d-1)/d}/\beta)$, as the level of interference is approximated by the product between home range overlap ($h_o = Nh$) and the pace of track reuse ($v \propto 1/\beta h^{1/d}$). Now, with $\beta \propto 1/h^{1/2d}$ from the invariance of local resource exploitation, we may rewrite regulation by interference as $f_\iota(Nh^{(2d-1)/2d})$. Thus, from the invariant argument we expect a $N \propto h^{(1-2d)/2d}$ relation where population density scales in proportion with the $-3/4$th and $-5/6$th power of the home range for two-dimensional versus three-dimensional ecological systems [l-plots, theoretical exponent of 1; observed of 0.40 (se:0.06; n:126) for birds, 0.98 (se:0.03; n:296) for placentals, & 0.63 (se:0.11; n:40) for marsupials].

The invariant amount of resource metabolised by populations ($Nw\beta \propto w^0$) is illustrated by the $1/N\beta \propto w$ relation in the m-plots [theoretical exponent of 1; observed of 0.83 (se:0.07; n:162) for birds, 1.18 (se:0.04; n:326) for placentals, & 0.80 (se:0.10; n:50) for marsupials]. We may thus for the invariant $Nh^{(d-1)/d}/\beta$ argument of interference regulation exchange N by $1/w\beta$ and obtain $h^{(d-1)/d}/w\beta^2$. This invariance implies proportionality between body mass and $h^{(d-1)/d}/\beta^2$, as illustrated for placentals in the second plot in Fig. 4 [theoretical exponent of 1; observed of 1.19 (se:0.07; n:74) for birds, 1.18 (se:0.03; n:190) for placentals, & 0.95 (se:0.11; n:23) for marsupials].

The two proportional relations $h^{1/d} \propto \beta^{-2}$ and $h^{(d-1)/d}/\beta^2 \propto w$—which reflect the invariances of the functional arguments for the regulation of foraging by local exploitation and interference competition (Fig. 4; 2 top plots)—contain the essential information that will give us the numerical values of the exponents of the mass-rescaling allometries. To see this we exchange home range and mass-specific metabolism with their mass-rescaling relations ($h \propto w^{\hat{h}}$ and $\beta \propto w^{\hat{\beta}}$), to obtain $w^{\hat{h}(d-1)/d} \propto w^{2\hat{\beta}+1}$ from the $h^{(d-1)/d}/w\beta^2 \propto w^0$ argument of interference regulation, and $w^{\hat{h}/d} \propto w^{-2\hat{\beta}}$ from the $\beta^2 h^{1/d} \propto w^0$ argument of local resource exploitation. This gives us the following two equations $\hat{h} = d(1+2\hat{\beta})/(d-1)$ and $\hat{h} = -2d\hat{\beta}$ for the allometric constraints on the foraging process. These equations are solved graphically for the allometric exponents $\hat{h} = 1$ and $\hat{\beta} = -1/2d$ in the third plot in Fig. 4.

	2D	3D	Ave	Pl 2D	Pl 3D	Mar	Bat
ϵ	.75	.83	$.69\,\frac{.04}{37}$	$.73\,\frac{.02}{60}$	-	-	-
$\underline{\beta}$	-.25	-.17	$-.33\,\frac{.01}{356}$	$-.29\,\frac{.01}{486}$	$-.14\,\frac{.02}{45}$	$-.25\,\frac{.01}{74}$	$-.21\,\frac{.02}{98}$
q_{ad}	-.25	-.17	$-.21\,\frac{.01}{829}$	$-.21\,\frac{.01}{140}$	$-.18\,\frac{.03}{39}$	$-.22\,\frac{.07}{14}$	$-.07\,\frac{.08}{15}$
m	-.25	-.17	$-.13\,\frac{.01}{1751}$	$-.25\,\frac{.01}{1203}$	$-.16\,\frac{.01}{331}$	$-.31\,\frac{.02}{182}$	$-.05\,\frac{.02}{366}$
R	.00	.00	$.10\,\frac{.01}{512}$	$-.06\,\frac{.02}{128}$	$.06\,\frac{.03}{37}$	$-.10\,\frac{.07}{14}$	$.02\,\frac{.08}{12}$
t_p	.25	.17	$.17\,\frac{0}{2224}$	$.24\,\frac{0}{1374}$	$.12\,\frac{0}{388}$	$.04\,\frac{.01}{156}$	$.13\,\frac{.02}{291}$
t_j	.25	.17	$.27\,\frac{.01}{1775}$	$.22\,\frac{0}{1226}$	$.10\,\frac{.02}{353}$	$.18\,\frac{.01}{168}$	$.21\,\frac{.02}{260}$
t_m	.25	.17	$.21\,\frac{.01}{1219}$	$.24\,\frac{.01}{1119}$	$.17\,\frac{.01}{357}$	$.11\,\frac{.02}{142}$	$.14\,\frac{.03}{185}$
t_r	.25	.17	$.21\,\frac{.01}{829}$	$.21\,\frac{.01}{140}$	$.18\,\frac{.03}{39}$	$.22\,\frac{.07}{14}$	$.07\,\frac{.08}{15}$
t_g	.25	.17	$.29\,\frac{.01}{450}$	$.31\,\frac{.02}{127}$	$.17\,\frac{.03}{39}$	$.27\,\frac{.13}{13}$	-
t_l	.25	.17	$.23\,\frac{.01}{1604}$	$.23\,\frac{0}{1404}$	$.12\,\frac{.01}{396}$	$.23\,\frac{.02}{183}$	$-.01\,\frac{.02}{217}$
N	-.75	-.83	$-.39\,\frac{.03}{1236}$	$-.80\,\frac{.02}{694}$	-	$-.33\,\frac{.06}{111}$	-
h	1.0	1.0	$1.13\,\frac{.07}{212}$	$1.14\,\frac{.04}{324}$	-	$.76\,\frac{.12}{44}$	$.16\,\frac{.19}{12}$

Table 2: **Allometric exponents** estimated from data. For birds (Ave), placentals minus bats (Pl) for 2D and 3D foraging, marsupials (Mar), and bats (Bat). The 2D and 3D columns list the theoretical exponents from Witting (1995, 2017a). Fraction numerators are se, and denominators n. Only $n > 11$ cases are shown.

The estimates of allometric exponents for raw data on birds, marsupials, bats, and 2D versus 3D placentals (minus bats) are listed in Table 2. The table includes also the predicted exponents from Witting (1995, 2017a) assuming that the inter-specific body mass variation follow from inter-specific variation in resource handling and density.

As expected for an ecological prediction, there is a general—but not complete—resemblance between the observed and predicted exponents. A 2D-3D-like transition is marked in placentals for all life history periods and ages, as well as for metabolism, mortality, and fecundity. The exponents for birds resemble a predominately 2D-ecological competition for territories and resources.

The metabolic exponent for bats resembles the 2D expectation, however, several of the exponents for bats deviate from the predicted, including a maximum lifespan exponent of -0.01 (se:0.02) and a home range exponent of 0.16 (se:0.19). These deviations identify a potential mismatch between the interactive ecology of bats and the foraging model behind the allometric deduction. Being based on intra-specific interactions in

overlapping home ranges of evenly distributed reproducing units, the foraging model was never intended to approximate the interactive ecology of gregarious bats that roots in large colonies. An extension with more elaborate models of interactive foraging is required to predict special cases.

9 Abundance & inter-specific competition

The allometric deduction predicts a change in abundance $[\partial \ln N^*/\partial \ln w = \hat{n}$, with $\hat{n} = (1-2d)/2d]$ following an evolutionary change in mass. While the prediction differs from the empirical scaling for birds and marsupials in Table 2, the abundance allometry is known to change with the scale of observation (Nee et al. 1991). This change is predicted by a scale-dependent adjustment of the inter-specific variation in population dynamic feedback selection.

The allometric deduction reflects the invariant resource bias ($\iota^{**}\psi$) across the individuals in the population. Yet the use of this invariance in the standard formulation for the allometric deduction of abundance contains the implicit assumption of an invariant resource gradient (ψ). This assumption seems fair on a scale where the partitioning of resources is unaffected by inter-specific competition, but it is a simplification when we examine allometries across competitive guilds.

Among the species of competitive guilds, we expect an inter-specific partitioning of resource by interactive competition, with the larger species having access to more resources than the smaller species. Assuming that the individuals of a species compete less per encounter when resources are abundant, this implies an inter-specific body mass dependence $\ln \psi \propto \hat{\psi} \ln w$ with a $\hat{\psi}$-exponent that declines from zero to some lower negative value with an increase from zero in the level of inter-specific resource partitioning. Now, from the $\iota \propto 1/\psi$ dependence of eqns 8 and 9 and the expected proportionality between abundance and the number of interactive encounters, we have $N \propto 1/\psi$. The expected change in abundance with body mass is thus

$$\frac{\partial \ln N^*}{\partial \ln w} = \hat{n} - \hat{\psi} \tag{10}$$

Nee et al. (1991) used the unusually good population size estimates of British and Swedish birds to examine the relationships between body mass and abundance. At the scale of all species—where we can expect a $\hat{\psi}$ exponent around zero owing to the general lack of competition between waterfowl, shorebirds, raptors, and passerines—Nee et al. (1991) estimated a partial $\partial \ln n^*/\partial \ln w$ relation of -0.75 among British birds, and -0.77 among Swedish, as predicted by a predominantly two-dimensional distribution of territories.

For comparisons across more closely related species, there were often positive relations between abundance and body mass in agreement with a strong partitioning of resources from inter-specific competition. Nee et al. (1991) did not quantify these relations, yet the $\hat{\psi}$ exponent needs to approach $-3/4$ to generate a positive relation. At the scale of the abundance data behind Table 2, we estimate a $\hat{\psi}$ exponent of inter-specific competition of about -0.36 and -0.42 for birds and marsupials, and no apparent inter-specific resource partitioning for placentals.

10 Primary selected metabolism

So far, we have considered the allometric effects of mass-rescaling only, which are the natural selection changes in the life history imposed by the natural selection of mass. Yet, there is an additional layer of metabolic-rescaling allometries that arise from the primary selection of mass-specific metabolism and the associated selection of mass and scaling of rate and time dependent life histories (Witting 2017a). Some of these effects are hidden below the surface of the traditional inter-specific allometries (Witting 2018), while others influence the inter-specific allometries among unicells (Witting 2017a), allometries on larger evolutionary scales (Witting 2017b), and allometries for body mass evolution in time (Witting 2020).

To include metabolic rescaling, we need to consider net energy in more detail. Net energy (ϵ) is obtained by multiplying

$$\epsilon = \alpha\beta \tag{11}$$

resource handling (α, including the resources themselves) with the pace (speed) of handling, with the latter reducing to a proportional measure of mass-specific metabolism (β, for details see Witting 2017a). The three traits are exposed to unconstrained selection for exponential increase (Witting 2020), and the theoretical body mass exponent for net energy $[\hat{\epsilon} = (2d-1)/2d]$ is special in the sense that it does not depend on the underlying cause (α versus β) for the generation of the net energy that is selected into body mass. This produces the following constraint

$$\hat{\epsilon} = \hat{\alpha} + \hat{\beta} = (2d-1)/2d \tag{12}$$

among the theoretical exponents for net energy, resource handling, and pace (Witting 2017a). The al-

lometric exponents

$$\hat{x} = \hat{x}_\beta + \hat{x}_w \tag{13}$$

of most traits (x), however, depend on the relative importance of metabolism for the selection of mass, with the final exponent ($\hat{x}$) being the sum of the two sub-exponents that evolve from the metabolic-rescaling ($\hat{x}_\beta$) and mass-rescaling ($\hat{x}_w$) selection of the life history (Witting 2017a).

For cases where none of the body mass variation arises from primary selected differences in metabolism we have $\hat{\beta}_\beta = 0$, and thus $\hat{\beta} = \hat{\beta}_w = -1/2d$ and $\hat{\alpha} = \hat{\epsilon} - \hat{\beta} = (2d-1)/2d + 1/2d = 1$. For the alternative limit case where all variation follows from primary selected differences in metabolism we have $\hat{\alpha} = 0$ and thus $\hat{\beta} = \hat{\epsilon} = (2d-1)/2d$ and $\hat{\beta}_\beta = \hat{\beta} - \hat{\beta}_w = (2d-1)/2d + 1/2d = 1$, as $\hat{\beta}_w = -1/2d$.

As birds and mammals have approximate mass-rescaling allometries with inter-specific $\hat{\beta}$ exponents around $-1/2d$, it follows that the primary cause for the evolutionary variation in net energy and body mass within each taxon is variation in resource handling. This makes sense as it would typically reflects evolutionary scenarios where the historical diversification of a taxon occurs by an evolutionary radiation across natural resources and niches, allowing for a relatively fast adaptation of resource handling that may easily outrun a background selection on mass-specific metabolism (which is expected to be slow for species with fully developed metabolic pathways). Net energy would then be strongly dependent on resource handling, as illustrated by the n-plots [exponent: 0.64 (se:0.03; n:37) for birds & 0.73 (se:0.01; n:68) for placentals]. This means that mass-specific metabolism declines with net energy because of the secondary downscaling from a body mass that increases with net energy [f-plots, exponent: -0.36 (se:0.05; n:32) for birds & -0.32 (se:0.02; n:64) for placentals].

Some fraction of the residual variation ($\beta/w^{-1/2d}$) in mass-specific metabolism (β) relative to mass-rescaling ($w^{-1/2d}$), however, should reflect differences in the primary selected metabolism. The residual net energy ϵ/α that is left over from the variation in resource handling should thus be positively dependent on the residual variation in β; as illustrated in the o-plots [exponent: 2.34 (se:0.38; n:32) for birds & 1.03 (se:0.29; n:64) for placentals].

Part of the body mass variation in birds and mammals are thus generated by primary selected differences in mass-specific metabolism. We may thus—if the span in net energy and body mass is generated by an invariant relative importance of resource handling and pace for the generation of net energy—expect from eqns 12 and 13 that the final mass-specific exponents ($\hat{\beta}$) are somewhat larger, i.e. less negative, than $-1/4$. Yet, the observed exponents are smaller, being -0.33 (se:0.01) for birds and -0.29 (se:0.01) for placentals.

The stronger than expected negative scaling of mass-specific metabolism shows that there is no invariant α/β ratio at this scale of observation. It is instead predominantly the smaller species that have larger mass-specific metabolisms, net energies, and body masses than expected from pure mass-rescaling, while the larger species tend to have smaller mass-specific metabolisms, net energies, and body masses relative to pure mass-rescaling selection. As shown by Witting (2018), this is exactly what we expect for an evolutionary taxon that diversities over long evolutionary timescales with a small body mass invariant primary selected rate of exponential increase in mass-specific metabolism, when measured on the per-generation timescales of the different species in the taxon.

An invariant primary selection of metabolism will generate an invariant exponential increase in mass-specific metabolism on the per-generation timescale of natural selection (Witting 2020). Yet, for the same rate of increase on the timescale of natural selection, metabolic evolution in physical time accelerates more in the smaller species because they evolve over a larger number of generations. By simulating the evolutionary radiation of placental and marsupial mammals from the extinction of dinosaurs, Witting (2018) found that this body mass dependent evolutionary acceleration bends the inter-specific metabolic allometry over time, with the primary selection of metabolism predicting a curvature in the metabolic allometry of placentals, as documented by Hayssen and Lacy (1985), Dodds et al. (2001), Packard and Birchard (2008), Kolokotrones et al. (2010), and MacKay (2011). The metabolic scaling for marsupials, on the other hand, showed almost no curvature suggesting that placentals have more primary selected variation in mass-specific metabolism than marsupials.

From the stronger acceleration of primary selected metabolism in the smaller species we expect a decline in the mass-rescaling residual for mass-specific metabolism ($\beta/w^{-1/2d}$) with an increase in mass, as illustrated in the p-plots not only for placentals but also for birds. With correlation coefficients of -0.21 ($p<0.001$; n:531) and -0.46 ($p<0.001$; n:356), and regression exponents of -0.03 (se:0.01; n:531) and -0.08 (se:0.01; n:356) for placentals and birds both relations are highly significant.

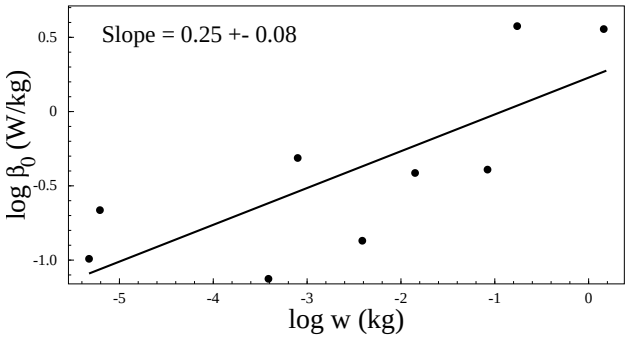

Figure 5: **Metabolic intercept.** The across taxa allometry for the intercepts ($\beta_\circ$) of the inter-specific allometries of mass-specific metabolism ($\beta = \beta_\circ w^{\hat{\beta}}$) in amphipods, crustacea, spiders, beetles, salamanders, fish, lizards, birds, and mammals (dots from left to right). Data from Peters (1983); w estimate of each taxon is the geometric midpoint of the mass range of the inter-specific allometry.

The decline in physical time in the selected acceleration of mass-specific metabolism with an increase in mass generates an increase in the exponent of total metabolism with an increase in mass, with the estimated exponent for placentals increasing from about 0.67 to 0.75 (Witting 2020). Yet, the observed exponent increases from about 0.67 to 0.87 (Kolokotrones et al. 2010).

The larger than predicted increase in the metabolic exponent of the largest placentals may reflect that these species evolve the smallest mass-specific metabolism from mass-rescaling. They may thus experience a more unconstrained selection of metabolism, with a larger per-generation increase, than the smaller species. This would explain not only the upward bend in the metabolic allometry for the largest placentals, but also the non-linearity of the residual distributions in the p-plots for placentals and birds. For placentals, we have a clear decline in residual mass-specific metabolism from the smallest to medium sized species, with an apparent increase in the larger species. The pattern in birds is less clear, yet there is a slight non-linearity where an initial decline is levelling off in the larger species.

In agreement with Witting (2018), a decline in the primary selected metabolism with an increase in mass could not be detected for marsupials, and nor for bats [correlation: -0.02 (p:0.84; n:74) for marsupials & 0.16 (p:0.11; n:98) for bats]. At least for marsupials, this agrees with an allometric exponent of -0.25 (se:0.01) for mass-specific metabolism, indicating pure mass-rescaling selection with practically no primary selected variation in mass-specific metabolism.

11 Selection of major taxa

Where the importance of primary selected metabolism is somewhat hidden as secondary effects of curvature in the inter-specific allometries of birds and mammals, it is more clearly expressed on the larger evolutionary scale across major taxonomic groups.

Considering allometric relations across taxa with approximate mass-rescaling allometries across the species of each taxon (as in birds and mammals), the importance of primary selection on mass-specific metabolism for the evolutionary divergence of taxa is captured by the allometric scaling of the intercepts ($\beta_\circ \propto w^{\hat{\beta}_\beta}$) of the inter-specific mass-rescaling allometries of the different taxa

$$\beta = \beta_\circ w^{\hat{\beta}_w} \tag{14}$$

Where the $\hat{\beta}_\beta$ exponent for the allometric scaling of the intercepts has a theoretical range from zero to unity (see Witting 2017b Fig. 3 for a graphical explanation). This exponent is estimated to 0.25 (se:0.08) across nine taxa of vertebrates (Fig. 5), corresponding with an invariant mass-specific metabolism across taxa ($\hat{\beta} = \hat{\beta}_w + \hat{\beta}_\beta = -0.25 + 0.25 = 0$) as concluded also by Makarieva et al. (2005, 2008), Kiørboe and Hirst (2014), and Witting (2017b).

The observed intercept scaling means that the evolutionary emergence of a new taxon occurs by a natural selection where the loss of mass-specific metabolism by the mass and mass-rescaling that follows from selected improvements in resource handling, is continuously being reselected by the background selection for an exponential increase in mass-specific metabolism. In other words, the selected restructuring of the base-phenotype from one taxon to another occurs so slowly that the background selection for increased metabolism keeps up with the pace of evolution, and thus maintains a fully developed mass-specific metabolism despite of mass-rescaling selection for a continuous decline in mass-specific metabolism. The evolution of new taxa occurs apparently along an upper limit on mass-specific metabolism, generating a succession of emerging taxa with increasingly higher metabolic intercepts, as observed across taxa of endotherms (Gavrilov et al. 2022).

The balance where primary selected metabolism outweigh the metabolic loss of mass-rescaling, has been estimated also at the macro evolutionary scale of maximum mass among all mobile organisms on Earth covering 3.5 billion years of evolution (Witting 2020). This corresponds with a log-linear exponential increase in physical time, reflecting a dw/dt-exponent of unity for the mass dependence of the rate of increase in mass in

physical time.

The full range of theoretical dw/dt-exponents has been identified for fossils of mammals (Witting 2020). At one end of the spectrum, the value is 3/4, and the relative importance of metabolic selection is negligible because of fast improvements in resource handling. This is observed for the evolution of maximum mass across all terrestrial mammals. At the other end, the value is 3/2 for within-niche evolution with optimal resource handling and a mass that increases from primary selected metabolism, as estimated for 60 million years of evolution in small horses.

Prokaryotes provide another example where a steep exponent of about 0.84 (DeLong et al. 2010) for mass-specific metabolism is predicted from body masses that are selected from primary variation in mass-specific metabolism (Witting 2017a,b). The positive exponent declines towards the well-known value of $-1/4$ for an increase in mass across protists and protozoa, as predicted by body masses that are selected beyond those of prokaryotes by the gradual unfolding of population dynamic feedback selection (Witting 2017a,b).

These examples illustrate that primary selected metabolism is of crucial importance for a deeper understanding of allometries.

12 Discussion

I have shown that the conceptually relatively simple model of population dynamic feedback selection explains a variety of observed allometric exponents, as well as underlying correlations connected to essential selection mechanisms. This includes some of the most well-known inter-specific exponents on a variety of life history and ecological traits, being explained primarily from the structural constraints on optimal foraging in predominantly two and three spatial dimensions. The prediction includes the broad range of alternative exponents listed by the five points in the introduction, with transitions explained primarily by metabolism selected at different scales of evolution.

Being introduced by the first formal deduction of 3/4 scaling in 1995, feedback selection was developed into a general life history and population dynamic theory (Witting 1997, 2008), being extended later by primary selection on mass-specific metabolism (Witting 2017a,b, 2018, 2020). All these components are based on the same population ecological model, and I have so far not been able to find any other theory that predicts the wide range of allometries, including the natural selection of metabolism and mass, and associated lifeforms of virus, prokaryotes, protists, and sexually reproducing multicellular animals. With the ecological model being developed for a base-case type of competition in spatial habitats, the foraging model allows for potential modifications that might explain alternative allometries, as observed e.g. among bats.

In judging different hypotheses, it is essential to realise the limitations of the theoretical frameworks applied. The widespread concept that it is possible to identify the cause of allometries by considering the scaling of metabolism exclusively, e.g., imposed a blind angle that prevented a distinction between realistic and unrealistic selection models. It is not only metabolism but the whole life history—as well as ecological traits like abundance and home range—that scale in allometric proportions with body mass. All these traits are essential components of populations, and thus part of the variation that generates natural selection. With minimal attention on the life history as a whole, it was not noted that metabolic scaling was explained by an unrealistic distortion in other life history components.

This distortion relates to the allometric hypotheses that do not explicitly incorporate the frequency-dependent selection among interacting replicators (which is basically all other hypotheses than population dynamic feedback selection). I refer collectively to these as physiological models, reflecting at least some degree of physiological optimisation in the absence of ecological interactions.

Physiological optimisation implies selection by the fundamental theorem of natural selection causing an increase in the average growth rate (r) and/or carrying capacity (k) of the population (Fisher 1930). In other words, physiological selections cannot—at least not in a straightforward way—select an increase in body mass that is associated with the observed decline in r and k.

The flawed positive scaling of r and k is usually ignored, maybe partially because many of the allometric hypotheses do not even consider the natural selection of mass. We are apparently so used to the existence of large-bodied organisms that they are taken for granted. But large body masses are not granted by physiological selection for the simple reason that the quality-quantity trade-off (Smith and Fretwell 1974; Stearns 1992) selects for the absence of mass. There are nevertheless several physiologically based studies on the selection of mass, individual growth, and associated allometries (e.g., Kozlowski and Weiner 1997; West et al. 2001; Brown and Sibly 2006; Bueno and López-Urrutia 2012; Kozlowski et al. 2020; White et al. 2022). Yet, these are contingent models where the selected masses and allometries follow from parameters and constraints that have evolved by natural selection

and are incorporated as assumptions into the models, instead of being explained from first principles of the structural constraints that cannot evolve. By fitting models to evolved phenotypes these methods illustrate how the different physiological components are interrelated, but they do not explain the cause for the selection of mass and allometries. If the contingent assumptions were allowed to evolve, the quality-quantity trade-off would dominate the physiological structure selecting a singularity with infinite replication, zero mass, and no allometries.

Population dynamic feed-back selection provides a promising way forward, away from the singularity of super-replicators with no mass. It selects life forms independently of contingent constraints, with large-bodied organisms selected by a density-dependent interactive competition that outbalances the downward pull of the quality-quantity trade-off. This selection is sufficient to get allometric theory going as it explains allometric exponents from the necessary population ecological structure, generating a balanced life history where r and k are selected to decline with an increase in mass.

Acknowledgements

I thank anonymous reviewers for helpful comments. All life history estimates, and associated population dynamic models, are available online at https://mrLife.org.

References

Banavar J. R., Damuth J., Maritan A., Rinaldo A. (2002). Modelling universality and scaling. Nature 420:626.

Banavar J. R., Maritan A., Rinaldo A. (1999). Size and form in efficient transportation networks. Nature 399:130–132.

Blum J. J. (1977). On the geometry of four-dimensions and the relationship between metabolism and body mass. J. theor. Biol. 64:599–601.

Browman H. I. (2000). Theme Section on 'Evolution' of fisheries science. MEPS 208:299–313.

Brown J. H. Sibly R. M. (2006). Life-history evolution under a production constraint. Proc. Nat. Acad. Sci. 103:17595–17599.

Bueno J. López-Urrutia A. (2012). The offspring-development-time/offspring-number trade-off. Am. Nat. 179:E196–E203.

Calder W. A. I. (1984). Size, function, and life history. Harvard University Press, Cambridge.

Capellini I., Venditti C., Barton R. A. (2010). Phylogeny and metabolic scaling in mammals. Ecology 91:2783–2793.

Carlson S. M., Edeline E., Vollestad A. L., Haugen T. O., Winfield I. J., Fletcher J. M., Ben James J., Stenseth N. C. (2007). Four decades of opposing natural and human-induced artificial selection acting on Windermere pike (*Esox lucius*). Ecol. Lett. 10:512–521.

Charlesworth B. (1971). Selection in density-regulated populations. Ecology 52:469–474.

Damuth J. (1981). Population density and body size in mammals. Nature 290:699–700.

Damuth J. (1987). Interspecific allometry of population density in mammals and other animals: the independence of body mass and population energy-use. Biol. J. Linnean Society. 31:193–246.

Darveau C.-A., Suarez K. S., Andrews R. D., Hochachka P. W. (2002). A general model for ontogenetic growth. Nature 417:166–170.

De Magalhães J. P. Costa J. (2009). A database of vertebrate longevity records and their relation to other life-history traits. J. Evol. Biol. 22:1770–1774.

del Hoyo, J., Elliot, A., Sargatal, J., & Christie, D. A., eds (1992–2011). Handbook of the birds of the world. Vol. 1–16. Lynx Edicions, Barcelona.

DeLong J. P., Okie J. G., Moses M. E., Sibly R. M., Brown J. H. (2010). Shifts in metabolic scaling, production, and efficiency across major evolutionary transitions of life. Proc. Nat. Acad. Sci. 107:12941–12945.

Demetrius L. (2003). Quantum statistics and allometric scaling of organisms. Physica 322:477–490.

DeSante D. F. Kaschube D. R. (2009). The monitoring avian productivity and survivorship (MAPS) program 2004, 2005, and 2006 report. Bird Pop. 9:86–169.

Dobzhansky T. (1973). Nothing in biology makes sense except in the light of evolution. Am. Bio. Teach. 35:125–129.

Dodds P. S., Rothman D. H., Weitz J. S. (2001). Re-examination of the "3/4-law" of metabolism. J. theor. Biol. 209:9–27.

Dreyer O. Puzio R. (2001). Allometric scaling in animals and plants. J. Math. Biol. 43:144–156.

Duncan R. P., Forsythe D. M., Hone J. (2007). testing the metabolic theory of ecology: allometric scaling exponents in mammals. Ecology 88:324–333.

Dunning J. B. (2007). Handbook of Avian Body Masses (2nd ed). CRC Press, Boca Raton.

Fenchel T. (1974). Intrinsic rate of natural increase: The relationship with body size. Oecologia 14:317–326.

Fisher R. A. (1930). The genetical theory of natural selection. Clarendon, Oxford.

Fujiwara N. (2003). Origin of the scaling rule for fundamental living organisms based on thermodynamics. BioSys. 70:1–7.

Garland T. (1983). Scaling the ecological cost of transport to body mass in terrestrial mammals. Am. Nat.

121:571–587.

Gavrilov V. M., Golubeva T. B., Warrack G., Bushuev A V. (2022). Metabolic scaling in birds and mammals: How taxon divergence time, phylogeny, and metabolic rate affect the relationship between scaling exponents and intercepts. Biology 11:1067.

Gill, F. & Donsker, D., eds (2014). International Ornithological Committee World Bird List (v 4.4). doi:10.14344/IOC.ML.4.4.

Ginzburg L. Damuth J. (2008). The space-lifetime hypothesis: viewing organisms in four dimensions, literally. Am. Nat. 171:125–131.

Glazier D. S. (2005). Beyond the '3/4-power law': variation in the intra- and interspecific scaling of metabolic rate in animals. Biol. Rev. 80:611–662.

Glazier D. S. (2008). Effects of metabolic level on the body size scaling of metabolic rate in birds and mammals. Proc. R. Soc. B. 22:821–828.

Glazier D. S. (2009). Metabolic level and size scaling of rates of respiration and growth in unicellular organisms. Funct. Ecol. 23:963–968.

Gompertz B. (1832). On the Nature of the Function Expressive of the Law of Human Mortality, and on a New Mode of Determining the Value of Life Contingencies. Phil. Trans. R. Soc. Lond. 123:513–585.

Griffiths D. (1977). Caloric variation in Crustacea and other animals. J. Anim. Ecol. 46:593–605.

Hatton I. A., Dobson A. P., Storch D., Galbraith E. D., Loreau M. (2019). Linking scaling laws across eukaryotes. Proc. Nat. Acad. Sci. 116:21616–21622.

Haugen T. O. Vøllestad L. A. (2001). A century of life-history evolution in grayling. Genetica 112:475–491.

Hayssen V. Lacy R. C. (1985). Basal metabolic rates in mammals: taxonomic differences in the allometry of BMR and body mass. Comp. Bioch. Physiol. 81A:741–754.

Herczeg G., Gonda A., Merilä J. (2009). Evolution of gigantism in nine-spined sticklebacks. Evolution 63:3190–3200.

Hudson L. N., Isaac N. J. B., Reuman D. C. (2013). The relationship between body mass and field metabolic rate among individual birds and mammals. J. Anim. Ecol. 82:1009–1020.

Jetz W., Sekercioglu C. H., Böhning-Gaese K. (2008). The worldwide variation in avian clutch size across species and space. PLOS Biol. 6:e303.

Jones K. E., Bielby J., Cardillo M., Fritz S. A., O'Dell J., Orme C. D. L., Safi K., Sechrest W., Boakes E. H., Carbone C., Connolly C., Cutts M. J., Foster K. J., Grenyer R., Habib M., Plaster C. A., Price S. A., Rigby E. A., Rist J., Teacher A., Binninda-Emonds O. R. P., Gittleman J. L., Mace G. M., Purvia A. (2009). PanTHERIA: a species-level database of life history, ecology, and geography of extant and recently extinct mammals. Ecology 90:2648.

Killen S. S., Atkinson D., Glazier D. S. (2010). The intraspecific scaling of metabolic rate with body mass in fishes depends on lifestyle and temperature. Ecol. Lett. 13:184–193.

Kiørboe T. Hirst A. G. (2014). Shifts in mass scaling of respiration, feeding, and growth rates across life-form transitions in marine pelagic organisms. Am. Nat. 183:E118–E130.

Kleiber M. (1932). Body and size and metabolism. Hilgardia 6:315–353.

Kolokotrones T., Savage V., Deeds E. J., Fontana W. (2010). Curvature in metabolic scaling. Nature 464:753–756.

Kooijman S. A. L. M. (2000). Dynamic energy and mass budgets in biological systems. Cambridge University Press, Cambridge.

Kozlowski J., Konarzewski M., Czarnoleski M. (2020). Coevolution of body size and metabolic rate in vertebrates: a life-history perspective. Biol. Rev. 95:1393–1417.

Kozłowski J. Weiner J. (1997). Interspecific allometries are by-products of body size optimization. Am. Nat. 149:352–380.

MacKay N. J. (2011). Mass scale and curvature in metabolic scaling. J. theor. Biol. 280:194–196.

Mahoney S. A. Jehl J. R. J. (1984). Body water content in marine birds. The Condor 86:208–209.

Makarieva A., Gorshkov V. G., Li B.-L. (2003). A note on metabolic rate dependence on body size in plants and animals. J. theor. Biol. 221:301–307.

Makarieva A. M., Gorshkov V. G., Bai-Lian L. (2005). Energetics of the smallest: do bacteria breathe at the same rate as whales. Proc. R. Soc. B. 272:2219–2224.

Makarieva A. M., Gorshkov V. G., Li B., Chown S. L., Reich P. B., Gavrilov V. M. (2008). Mean mass-specific metabolic rates are strikingly similar across life's major domains: Evidence for life's metabolic optimum. Proc. Nat. Acad. Sci. 105:16994–16999.

McCarthy M. A., Citroen R., McCall S. C. (2008). Allometric scaling and Bayesian priors for annual survival of birds and mammals. Am. Nat. 172:216–222.

McKechnie A. E. Wolf B. O. (2004). The allometry of avian basal metabolic rate: Good predictions need good data. Physiolo Biochem Zool 77:502–521.

McNab B. K. (2008). An analysis of the factors that influence the level and scaling of mammalian BMR. Comp. Bioch. Physiol. A 151:5–28.

Myhrvold N. P., Baldridge E. amd Chan B., Sivam D., Freeman D. L., Ernest S. K. M. (2015). An amniote life-history database to perform comparative analyses with birds, mammals, and reltiles. Ecology 96:3109.

Nasrinpour H. R., Reimer A. A., Friesen M. R., McLeod R. D. (2017). Data preparation for West Nile Virus agent-based modelling: protocol for processing bird population estimates and incorporating ArcMap in

AnyLogic. JMIR Res Protoc 6:e138.

Nee S., Read A. F., Greenwood J. J. D., Harvey P. H. (1991). The relationship between abundance and body size in british birds. Nature 351:312–313.

Niven J. E. Scharlemann J. P. W. (2005). Do insect metabolic rates at rest and during flight scale with body mass? Biol. Lett. 1:346–349.

Odum E. P., Marshall S. G., Marples T. G. (1965). The caloric content of migrating birds. Ecology 46:901–904.

Olsen E. M., Heino M., Lilly G. R., Morgan M. J., Brattey J., Ernande B., Dieckmann U. (2004). Maturation trends indicative of rapid evolution preceded the collapse of northern cod. Nature 428:932–935.

Packard G. C. Birchard G. F. (2008). Traditional allometric analysis fails to provide a valid perdictive model for mammalian metabolic rates. J. Exp. Biol. 211:3581–3587.

Pearl R. (1928). The rate of living. Alfred A. Knopf, New York.

Prothero J. W. (2015). The design of mammals. A scaling approach. Cambridge University Press, Cambridge.

Rau A. R. P. (2002). Biological scaling and physics. J. Biosci. 27:475–478.

Reznick D. N., Butler I. M. J., Rodd F. H., Ross P. (1996). Life-history evolution in guppies (*Poecilia reticulata*) 6. differential mortality as a mechanism for natural selection. Evolution 50:1651–1660.

Ricklefs R. E., Tsunekage T., Shea R. E. (2011). Annual adult survival in several new world passerine birds based on age ratios in museum collections. J. Ornithol. 152:481–495.

Rossetto M., De Leo G., Bevacqua D., Micheli F. (2012). Allometric scaling of mortality rates with body mass in abalones. Oecologia 168:989–996.

Roughgarden J. (1971). Density-dependent natural selection. Ecology 5:453–468.

Rubner M. (1883). Über den einfluss der korper grosse auf stoff-und kraft-wechsel. Z. Biol. 19:535–562.

Santillán M. (2003). Allometric scaling law in a simple oxygen exchanging network: possible implications on the biological allometric scaling laws. J. theor. Biol. 223:249–257.

Santini L., Isaac N. J. B., Ficetola G. F. (2018). TetraDENSITY: A database of population density estmates in terrestrial vertebrates. Global Ecol. Biog. 27:787–791.

Sieg A. E., O'Connor M. P., McNair J. N., Grant B. W., Agosta S. J., Dunham A. E. (2009). Mammalian metabolic allometry: do intraspecific variation, phylogeny, and regression models matter? Am. Nat. 175:720–733.

Sinclair A. F., Swain D. P., Hanson J. M. (2002). Disentangling the effects of size-selective mortality, density, and temperature on length-at-age. Can. J. Fish. Aquat. Sci. 59:372–382.

Smith C. C. Fretwell S. D. (1974). The optimal balance between size and number of offspring. Am. Nat. 108:499–506.

Smith F. A., Brown J. H., Haskell J. P., Alroy J., Charnov E. L., Dayan T., Enquist B. J., Ernest S. K. M., Hadly E. A., Jablonski D., Jones K. E., Kaufman D. M., Lyons S. K., Marquet P., Maurer B. A., Niklas K., Porter W., Roy K., Tiffney B., Willig M. R. (2004). Similarity of mammalian body size across the taxonomic hierarchy and across space and time. Am. Nat. 163:672–691.

Stearns S. C. (1992). The evolution of life histories. Oxford University Press, Oxford.

Tamburello N., Cote I. M., Dulvy N. K. (2015). Energy and the scaling of animal space use. Amazoniana 186:196–211.

Tucker M. A., Ord T. J., Rogers T. L. (2014). Evolutionary predictors of mammalian home range size: body mass, diet and the environment. Global Ecol. Biog. 23:1105–1114.

West G. B., Brown J. H., Enquist B. J. (1997). A general model for the origin of allometric scaling laws in biology. Science 276:122–126.

West G. B., Brown J. H., Enquist B. J. (1999). The fourth dimension of life: fractal geometry and allometric scaling of organisms. Science 284:1677–1679.

West G. B., Brown J. H., Enquist B. J. (2001). A general model for ontogenetic growth. Nature 413:628–631.

White C. R., Alton L. A., Bywarter C. L., Lombardi E. J., Marshall D. J. (2022). Metabolic scaling is the product of life-history optimization. Science 377:834–839.

White C. R., Blackburn T. M., Seymour R. S. (2009). Phylogenetically informed analysis of the allometry of mammalian basal metabolic rate supports neither geometric nor quarter-power scaling. Evolution 63:2658–2667.

White C. R., Cassey P., Blackburn T. M. (2007). Allometric exponents do not support a universal metabolic allometry. Ecology 88:315–323.

Wilson, D. E. & Mittermeier, R. A., eds (2009–2014). Handbook of the mammals of the world. Vol. 1–4. Lynx Edicions, Barcelona.

Wilson, D. E. & Reeder, D. M., eds (2005). Mammals Species of the World. A Taxonomic and Geographic Reference (3rd ed). Johns Hopkins University Press, Baltimore.

Witting L. (1995). The body mass allometries as evolutionarily determined by the foraging of mobile organisms. J. theor. Biol. 177:129–137, https://doi.org/10.1006/jtbi.1995.0231.

Witting L. (1997). A general theory of evolution. By means of selection by density dependent competitive interactions. Peregrine Publisher, Århus, 330 pp, URL https://mrLife.org.

Witting L. (2002). From asexual to eusocial reproduction by multilevel selection by density dependent competitive interactions. Theor. Pop. Biol. 61:171–195,

https://doi.org/10.1006/tpbi.2001.1561.

Witting L. (2007). Behavioural interactions selecting for symmetry and asymmetry in sexual reproductive systems of eusocial species. Bull. Math. Biol. 69:1167–1198, https://doi.org/10.1007/s11538–006–9112–x.

Witting L. (2008). Inevitable evolution: back to *The Origin* and beyond the 20th Century paradigm of contingent evolution by historical natural selection. Biol. Rev. 83:259–294, https://doi.org/10.1111/j.1469–185X.2008.00043.x.

Witting L. (2017a). The natural selection of metabolism and mass selects allometric transitions from prokaryotes to mammals. Theor. Pop. Biol. 117:23–42, https://dx.doi.org/10.1016/j.tpb.2017.08.005.

Witting L. (2017b). The natural selection of metabolism and mass selects lifeforms from viruses to multicellular animals. Ecol. Evol. 7:9098–9118, https://dx.doi.org/10.1002/ece3.3432.

Witting L. (2018). The natural selection of metabolism explains curvature in allometric scaling. Oikos 127:991–1000, https://dx.doi.org/10.1111/oik.05041.

Witting L. (2020). The natural selection of metabolism explains curvature in fossil body mass evolution. Evol. Biol. 47:56–75, https://dx.doi.org/10.1007/s11692–020–09493–y.

Witting L. (2021). Life histories of 9,488 bird and 4,865 mammal species. Preprint at bioRxiv https://dx.doi.org/10.1101/2021.11.27.470200.